Available online at www.sciencedirect.com
SciVerse ScienceDirect
Physics Procedia 27 (2012) 240 – 243
Physics Procedia

ISS2011

Flux pinning properties of YBCO films with nano-particles by TFA-MOD method

Y. Masuda[a*], R. Teranishi[a], M. Matsuyama[a], K. Yamada[a], T. Kiss[b], S. Munetoh[a], M. Yoshizumi[c], T. Izumi[c]

[a]*Department of Materials Science and Engineering, Kyushu University, 744 Motooka, Nishi-ku, Fukuoka 819-0395, Japan*
[b]*Department of Electrical and Electronic Engineering, Kyushu University, 744 Motooka, Nishi-ku, Fukuoka 819-0395, Japan*
[c]*Superconductivity Research Laboratory – ISTEC, 1-10-13 Shinonome, Koto-ku, Tokyo 135-0062, Japan*

Abstract

Nano-particles were doped into YBCO films as pinning centers by a metal organic deposition (MOD) method using trifluoroacetates. Two types of initial solution with a cation ratio of Y: Ba: Cu = 1: 1.5: 3 were prepared; one with the dispersion of SnO_2 particles with the size of 15-25 nm and the other one with the dispersion of smaller ZrO_2 particles with the size of under 8 nm, then the solution was spin-coated on $CeO_2/Gd_2Zr_2O_7$/Hastelloy substrates. The coated films were calcined at 430 ºC in oxygen atmosphere and crystallized at 780 ºC in low oxygen atmosphere. From the results of X-ray diffraction analysis (XRD), peaks of $BaSnO_3$ were observed clearly in the YBCO film by the starting solution with SnO_2. On the other hands, little peaks corresponding to $BaZrO_3$ were observed in the film by the solution with ZrO_2. Many CuO segregations were recognized at the surface of SnO_2 doped YBCO film in comparison to the YBCO film with ZrO_2 doping. From these results, it is indicated that most of SnO_2 particles in precursors are react with Ba during heating. Critical current density (J_C) of the YBCO films by both solutions showed higher performance than that of pure YBCO film in magnetic fields.

Keywords: $YBa_2Cu_3O_{7-\delta}$ films; TFA; MOD; Flux pinning

1. Introduction

$REBa_2Cu_3O_{7-d}$ (REBCO, RE: rare earth elements) films have high critical current density (J_C), high transition temperature (T_C), and high irreversibility field (H_{irr}) so that these films are expected for applying superconducting wire. Metal organic deposition using trifluoroacetates (TFA-MOD) method is a promising procedure for YBCO films since this method can provide high superconducting properties in a cost-effective process with non-vacuum system [1–4]. However, J_C of YBCO films decreases in magnetic fields (**B**). So, in order to improve J_C in magnetic fields, various methods have been proposed for the introduction of effective artificial pinning centers (APCs) in superconducting films. It has been actually reported that J_C-**B** properties improved for REBCO films with $BaZrO_3$ particles of about 30 nm in diameter by the TFA-MOD method using a starting solution with dissolved Zr-salts [5-6]. Also, in our previous report, SnO_2 compounds were formed in the YBCO film with the size of about 30 nm by this method using a solution with dispersed SnO_2 particles and acted as pinning centers [7-8]. However, it is important to obtain higher J_C in

* Corresponding author. Tel.: +81-92-802-2970 ; fax: +81-92-802-2970 .
E-mail address: masuda@zaiko14.zaiko.kyushu-u.ac.jp .

1875-3892 doi:10.1016/j.phpro.2012.03.455

magnetic fields for the electric power application, so higher number density of particles with smaller size is considered to be effective pinning centers in this method. In this study, we fabricated YBCO films by a starting solution with ZrO_2 particles which have the size of about under 8 nm and investigated the growth process of YBCO film with nano-particles.

2. Experimental

YBCO films were fabricated by the TFA-MOD process. Starting solutions were prepared by dissolving Y-, Cu-octyl salts, and Ba-trifluoroacetates in an adequate solvent with a total metal ion concentration of 1.3 mol/L. We prepared two kinds of initial solutions which nano-particles were dispersed as pinning centers in; one with the dispersion of SnO_2 particles with the size of 15-25 nm, the other one with the dispersion ZrO_2 (Yttria-stabilized zirconia) with the size of under 8 nm. These particles were dispersed into the solution with the ratio of 2 mol%. The molar ratio of total metals in the solution is Y: Ba: Cu: M (M: Sn, Zr) = 1: 1.5: 3: 0.11. These solutions were deposited on $CeO_2/Gd_2Zr_2O_7$/Hastelloy substrates by a spin coating method at 3000 rpm for 120s. Then, two-step heat treatment was applied to the coated films. In the calcination step, these films were calcined up to 430°C at a heating rate of 5°C /min in oxygen atmosphere with water vapor of 2 vol.%. In order to fabricate thick precursor films, a process of coating and calcination were repeated for 3 times. Then, the calcined films were crystallized at a heating rate of 5°C /min and kept the maximum heating temperature of 780°C for 100 min in humid of 10 vol.% and low oxygen of 1000 ppm. Thickness of YBCO films were about 500-700 nm. Crystallinity of the films was characterized by XRD θ/2θ scan. The surface morphology of films was observed by scanning electron microscopy (SEM) and SEM-EDX (Energy Dispersive X-ray Spectroscopy) to analyze the microstructure and composition of the films. The superconducting properties of YBCO films were measured by a DC four probe method.

3. Results and discussion

3.1. Crystallized phases in YBCO films

The result of XRD θ/2θ scan for YBCO films with 2 mol% nano-particles are shown in Fig 1. The vertical axis in the figure shows peak intensities which divided by the peak intensity of CeO_2 (200). The result of pure YBCO film was described as a reference in the figure. The peaks of SnO_2 (110) , $BaSnO_3$ (110) and $BaSnO_3$ (200) were detected at 26.5°, 30°, and 42.5°, respectively, in SnO_2 added YBCO film. In the film with ZrO_2 addition, the peaks of ZrO_2 (111) and $BaZrO_3$ (200) were detected at 30° and 43°, respectively. In addition, the peak of $Y_2Cu_2O_5$ (211) and CuO (111) were detected in both films with nano-particles addition at 31° and 35°, respectively.

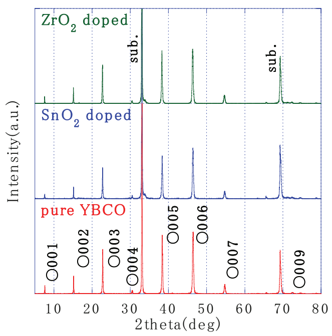

Fig. 1. XRD θ/2θ scan of YBCO films with 2 mol% SnO_2 and ZrO_2 addition.

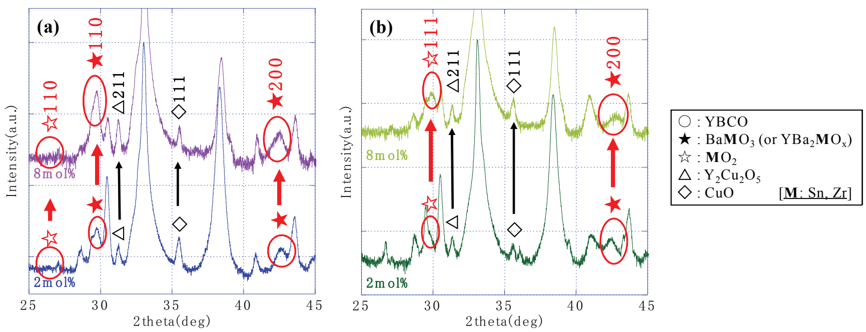

Fig. 2. XRD θ/2θ scan of YBCO films with 8 mol% (a) SnO_2 and (b) ZrO_2 addition.

In order to investigate differences of products in each film, higher concentration of particles were introduced to the starting solution and then YBCO films were fabricated. The result of comparison between 2 mol% particles doped film and 8 mol% doped one is shown in Fig 2. In SnO_2 doped films as shown in Fig 2(a), the phases of SnO_2, $BaSnO_3$, $Y_2Cu_2O_5$, and CuO were detected. Among them, large increments of peak intensities for $BaSnO_3$, $Y_2Cu_2O_5$ and CuO peak were confirmed as the concentration increase of SnO_2, but no increment was detected in SnO_2 peak. From these results, it is considered that the most of SnO_2 particles were combined with Ba and then changed to $BaSnO_3$ during heat treatment. While, the phases of ZrO_2, $BaZrO_3$, $Y_2Cu_2O_5$, and CuO were detected in the YBCO film ZrO_2 doped as shown in Fig 2(b). Among them, large increment for ZrO_2 peak and small increment for $Y_2Cu_2O_5$ and CuO peaks were observed with the increase of ZrO_2 addition, but the peak of $BaZrO_3$ was hardly increased. Thus, it is suggested that many ZrO_2 particles in precursors exist as same composition even after heating.

3.2. Surface morphology

To discuss the surface morphology of YBCO films with nano-particles doped, we observed the surface of YBCO films by SEM. Fig 3 shows the SEM images of surface for YBCO films. In the pure YBCO film as shown in Fig 3(a), *c*-axis oriented YBCO crystals were observed. In SnO_2 doped film as shown in Fig 3(b), segregation of particles with the diameter of about 1 μm was observed on the surface. On the other hand, segregation of particles was detected slightly on the surface for YBCO film with ZrO_2 addition as shown in Fig 3(c).

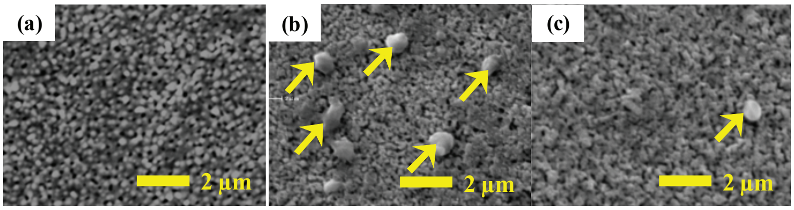

Fig. 3. SEM images of film surface for (a) pure YBCO, (b) YBCO with SnO_2 addition, and (c) YBCO with ZrO_2 addition.

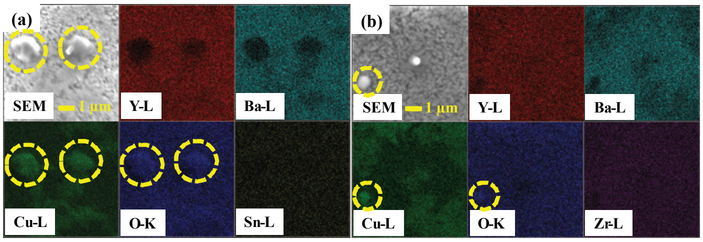

Fig. 4. SEM-EDX mapping images of YBCO films with (a) SnO_2 2 mol% addition and (b) ZrO_2 2 mol% addition.

In order to clarify the compositional element for these segregated precipitates as seen in Fig 3(b) and (c), SEM-EDX measurement for element mapping was performed. As shown in Fig 4(a) and (b), Cu oxide is observed where particles existed on the surface of both SnO_2 doped film and ZrO_2 doped one. Especially, much Cu oxide particles were observed for YBCO film with SnO_2 addition. From the results both XRD measurement and surface morphology observation, it can be considered that many CuO particles were remained for YBCO film with SnO_2 addition because of the result of reaction between SnO_2 and Ba during heat treatment. On the other hand, less CuO particles were observed for YBCO film with ZrO_2 addition, suggesting less ZrO_2 react with Ba during heating.

3.3. Superconducting properties

Fig 5 shows T_C values of pure YBCO films and YBCO films with 2 mol% nano-particles. T_C of YBCO films with SnO_2 and ZrO_2 addition were 90.7 K and 91.5 K, respectively, in comparison to pure YBCO film, 91.8 K. It is indicated that no degradation of T_C was recognized in YBCO films by introducing nano-particles.

Fig 6 shows dependences of J_C on magnetic field for pure YBCO film and YBCO films with 2 mol% nano-particles addition in magnetic field applied parallel to *c*-axis (**B**//*c*) at 77 K. J_C in self field ($J_C^{s.f.}$) of SnO_2 doped film and ZrO_2 doped one were 2.9 MA/cm^2 and 3.6 MA/cm^2, respectively, in comparison to pure YBCO film, 4.5 MA/cm^2. J_C in 3 T of SnO_2 doped was 0.14 MA/cm^2, and that of ZrO_2 doped film was 0.07 MA/cm^2. J_C of both YBCO films with nano-particles added was enhanced in comparison to pure YBCO in low magnetic field. And J_C of SnO_2 doped film was higher than pure YBCO in all magnetic fields. As a result, it is suggested that nano-particles doped in YBCO films acted as pinning centers.

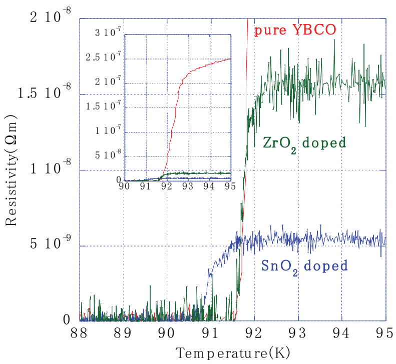

Fig. 5. T_C behavior of YBCO films with 2 mol% nano-particles addition.

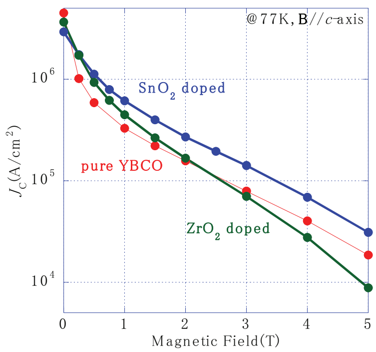

Fig. 6. J_C in magnetic fields at 77 K in **B**//*c*-axis.

3.4. Growth process of YBCO with nano-particles

According to the previous research [7-8], it was predicted that SnO_2 in precursors dissolved temporality during heat treatment and then combined with Ba to be $BaSnO_3$. By based on this predict, it was expected that similar tendency was also seen strongly in the case of smaller particles as the reaction from ZrO_2 to $BaZrO_3$. However, as seen in results of Fig 3 and Fig 4, the formation of $BaZrO_3$ was hardly confirmed in case of ZrO_2 addition. Therefore, it is considered that $BaSnO_3$ particles were formed not by the process of decomposing SnO_2 but by peritectic reaction between SnO_2 and Ba during heating.

On the other hand, ZrO_2 nano-particles could be expected for introducing smaller APCs in YBCO film. It is under investigating the effect of higher concentration addition of nano-particles into YBCO films and the optimization of crystallization conditions. Also, it is important to observe microstructures for identification of APCs in YBCO films in detail.

4. Conclusion

YBCO films were grown by a MOD process using TFA initial solutions containing nano-particles such as SnO_2 and ZrO_2 as pinning centers to investigate the growth process of YBCO film with nano-particles. It is considered that most of SnO_2 particles in precursors react with Ba and form $BaSnO_3$ during heat treatment. J_C in magnetic fields of SnO_2 doped film was enhanced in comparison to pure YBCO film. In order to obtain higher J_C in magnetic fields, it is necessary to control doping concentration of nano-particles into YBCO films and to optimize crystallization condition.

Acknowledgements

This work was supported by the New Energy and Industrial Technology Development Organization (NEDO) through International Superconductivity Technology Center (ISTEC). The authors are grateful to Prof. Y. Yoshida and Prof. Y. Ichino (Nagoya Univ.) and Prof. S. Awaji (Tohoku Univ.) for their support on superconducting property measurements.

References

[1] A. Gupta, R. Jagannathan, E. I. Cooper, E. A. Giess, J. I. Landman, B. W. Hussey, Appl. Phys. Lett. 52 (1988) 2077.

[2] P. C. McIntyre, M. J. Cima, M. F. Ng, J. Appl. Phys. 68 (1990) 4183

[3] P. C. McIntyre, M. J. Cima, J. A. Smith Jr., R. B. Hallock, M. P. Siegal, J. M. Philips, J. Appl. Phys. 71 (1992) 1868.

[4] T. Araki, K. Yamagiwa, K. Suzuki, I. Hirabayashi, S. Tanaka, Supercond. Sci.Technol. 14 (2001) L21.

[5] X. Obradors, T. Puig, A. Pomar, F. Sandiumenge, N. Mestres, M. Coll, et al, Supercond. Sci. Technol. 19 (2006) S13.

[6] M. Miura, T. Kato, M. Yoshizumi, Y. Yamada, T. Izumi, T. Hirayama, Y. Shiohara, Applied Physics Express 2 (2009) 023002.

[7] Y. Miyanaga, R. Teranishi, K. Yamada, N. Mori, M. Mukaida, T. Kiss, et al, Physica C 469 (2009) 1418-1421

[8] R. Teranishi, Y, Miyanaga, K. Yamada, N. Mori, M. Mukaida, M. Inoue, et al, J. Phys.: Conf. Ser. 234 (2010) 022039.